Geologie en Mijnbouw **73:** 331–337, 1994.

Accelerometer recordings of the 1992 Roermond earthquake, the Netherlands, and ground motion simulations using the empirical Green's function method

J.A. Helm, M. Bour* & P. Hoang-Trong
*Ecole et Observatoire de Physique du Globe, 5 rue René Descartes, 67084 Strasbourg Cedex, France; * present address: B.R.G.M., 117 Avenue de Luminy, 13009 Marseille, France*

Received 16 August 1993; accepted in revised form 18 February 1994

Key words: peak ground acceleration, Roermond earthquake, empirical Green's function

Abstract

A telemetered digital three-station network at Soultz-sous-Forêts in NE France (280 km SE of Roermond) recorded the M_L = 5.8 mainshock of the Roermond earthquake on April 13, 1992 and also the M_L = 3.6 aftershock at 01:06 UTC, April 14, 1992.

Using the empirical Green's function method the ground motions recorded during the mainshock are modelled from the recording of the aftershock. This method is used to calculate a maximum ground acceleration of 0.17 m/s^2 (peak-to-peak) at a site in the Rhine Graben where the observed maximum ground acceleration was 0.18 m/s^2. The recordings from the three stations show a variation in the amplitude of peak-to-peak ground acceleration for the three sites, from 0.027 m/s^2 at a rock site on the edge of the Upper Rhine Graben to 0.18 m/s^2 at a station on sediments in this graben.

The recording network

The three-station recording network installed in the framework of the European Hot Dry Rock project at Soultz-sous-Forêts is described in Table 1 and the geographical location of the network relative to Roermond is shown in Fig. 1. One station, Langenberg, is situated in the N. Vosges on the edge of the Upper Rhine Graben, while the other two, Hoffen and Surbourg are in the graben.

The records

The arrival of the P-waves from the M_L = 5.8 mainshock of April 13, triggered the recording system. However, the seismometers at all stations were saturated by the arrival of the surface waves. The ground motions caused by the surface waves (Lg and Rg) were recorded on the accelerometers. The maximum peak-to-peak acceleration was 0.18 m/s^2 recorded on the E-W and N-S components at Surbourg. At Hoffen the maximum accelerations were 0.08 m/s^2 and 0.06 m/s^2 on the N-S and E-W component, respectively (Fig. 2). Figure 3 shows a comparison of the maximum peak-to-peak vertical accelerations at the three stations: Langenberg 0.03 m/s^2 on a rock site, Hoffen 0.04 m/s^2 and Surbourg 0.05 m/s^2, both on Quaternary sediments.

The following day the M_L = 3.6 aftershock at 01:06 UTC was also recorded by the network. This aftershock has since been considered as a triggered event (Ahorner 1994), with an epicenter 30 km SE of Roermond. These two records were considered suitable for an application of the empirical Green's function method for modelling ground motion.

Modelling of the ground motion

The empirical Green's function method

In regions where records of small earthquakes are available from local networks the method of the empirical Green's function, proposed more than a decade ago by

Table 1. Details of the three stations of the permanent recording network at Soultz-sous-Forêts in the Upper Rhine Graben. This network operates within the European Hot Dry Rock (HDR) project.

Station	Langenberg	Hoffen	Surbourg
Latitude	48°58′50″N	48°56′30″N	48°54′53″N
Longitude	7°48′19″E	7°57′50″E	7°51′ 8″E
Elevation	+ 500 m	+ 150 m	+ 200 m
Site geology	Triassic	Quaternary	Quaternary
	L. Vosges Sandstone	Loess	Loess
Instrumentation	3-component	3-component	3-component
	Kinemetrics SS-1 Ranger	Sundstrand QA-700	Sundstrand QA-700
	seismometer,	accelerometer,	accelerometer,
	1 vertical component	1 vertical component	1 vertical component
	Sundstrand QA-700	Kinemetrics SS-1 Ranger	Kinemetrics SS-1 Ranger
	accelerometer	seismometer	seismometer

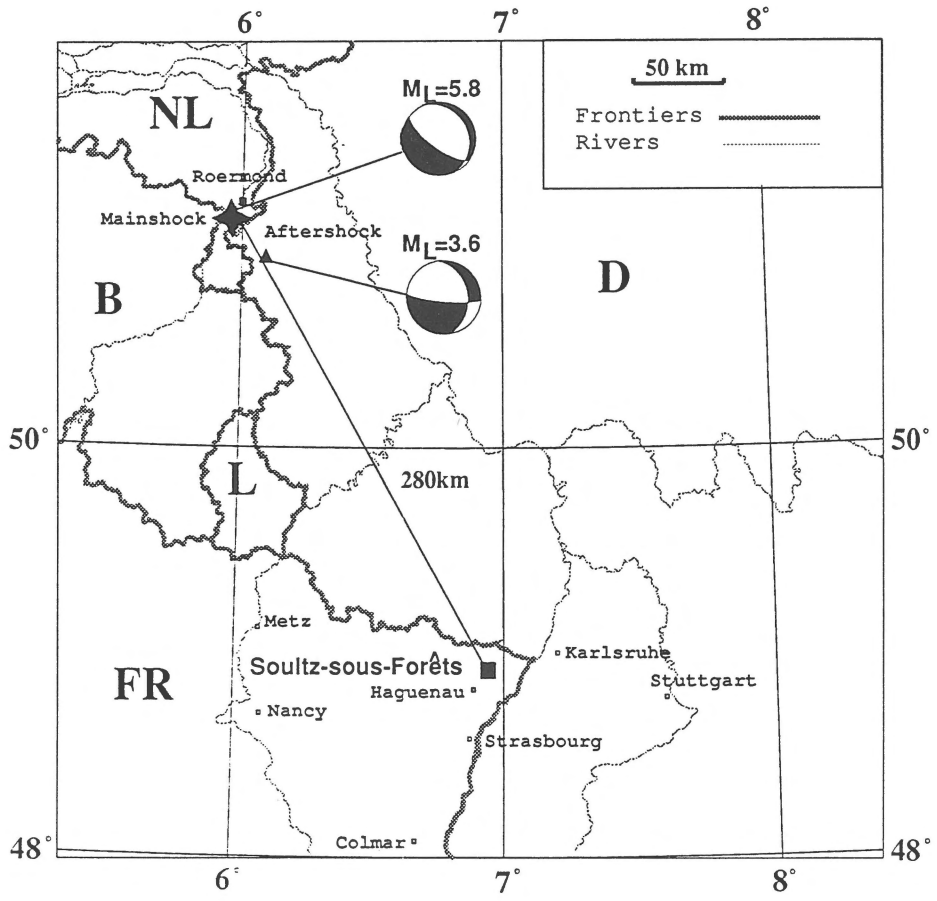

Fig. 1. Location of Soultz-sous-Forêts relative to Roermond. The focal mechanisms (lower hemisphere projection) of the mainshock (M_L = 5.8) and the aftershock (M_L = 3.6), used as an empirical Green's function, are shown.

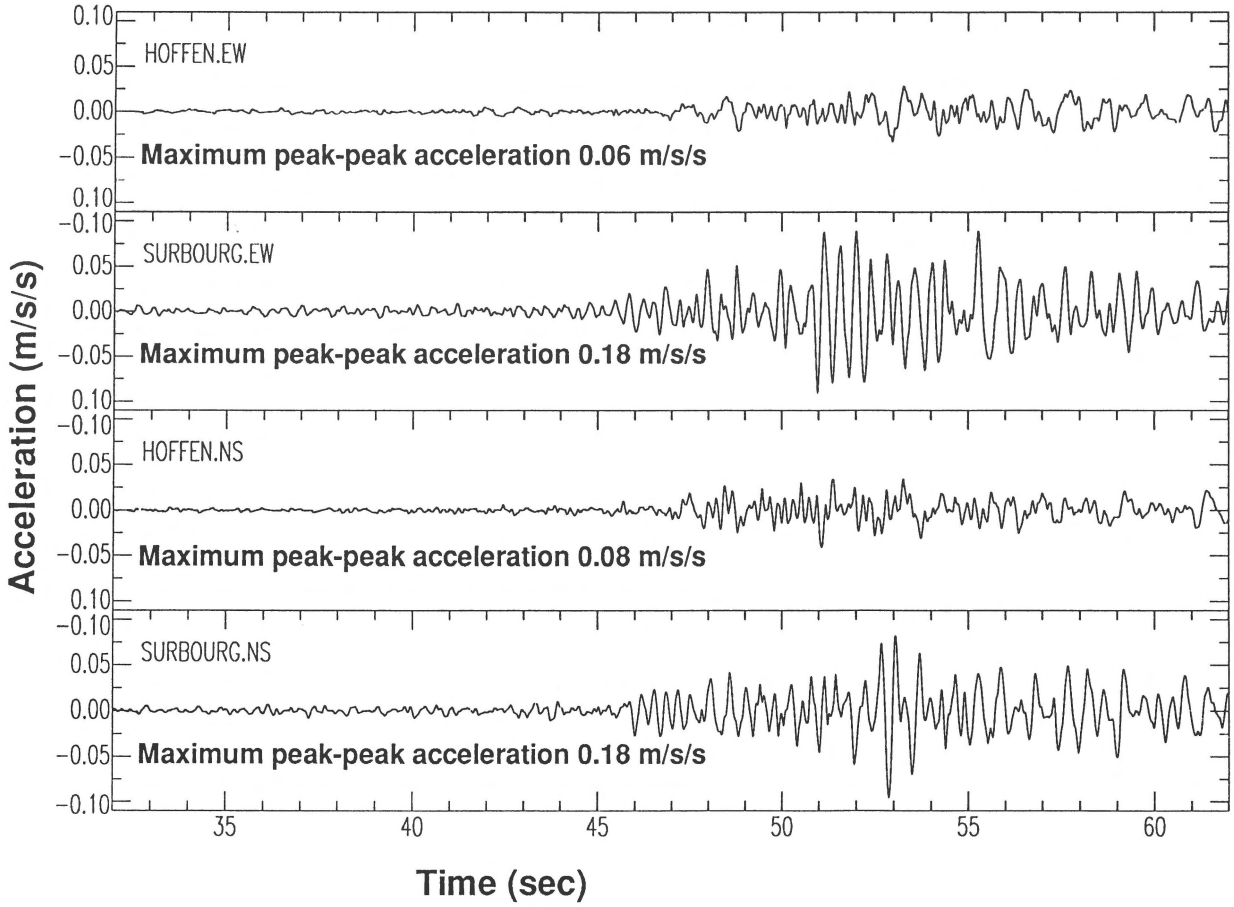

Fig. 2. Horizontal component accelerometer recordings of the Roermond earthquake at Surbourg and Hoffen.

Hartzell (1978), may be particularly useful for predicting strong motion accelerations. The empirical Green's functions are made up from the records of small events, which describe the seismic wave propagation through the real structure of the Earth. In the far field approximation, the method consists principally of summing these functions to simulate the ground motions that could be produced by a larger seismic source. Details of this method are explained by Bour & Cara (1995). In regions of moderate to low seismicity, the rate of occurrence of magnitude 5.8 to 6.0 earthquakes may be so small that the chance to record strong ground motion is very low, while small earthquakes may well be recorded locally. Very few accelerometer data are indeed available to earthquake engineers in regions of moderate seismicity like northwestern Europe, where seismic risk is nevertheless significant as a result of the high population density and of heavily developed industrialization. The empirical Green's function method, which is aimed at estimating the ground motion due to a large earthquake as a sum of small event records, is very well suited for simulating strong ground motions in such situations.

By using recorded ground motions as empirical Green's functions, wave propagation and local site effects are implicitly included, since the motions observed from the small event records already contain this information. On the other hand, the source excitation functions are computed theoretically for a given set of source parameters. The application of this method requires several simplifying assumptions: linearity, validity of the far field approximation, the same focal mechanisms for the small event as the large earthquake, and the same travel paths between the station and the fault surface elements of the large earthquake.

In order to determine the number of fault elements representing the main event fault plane, self-similarity

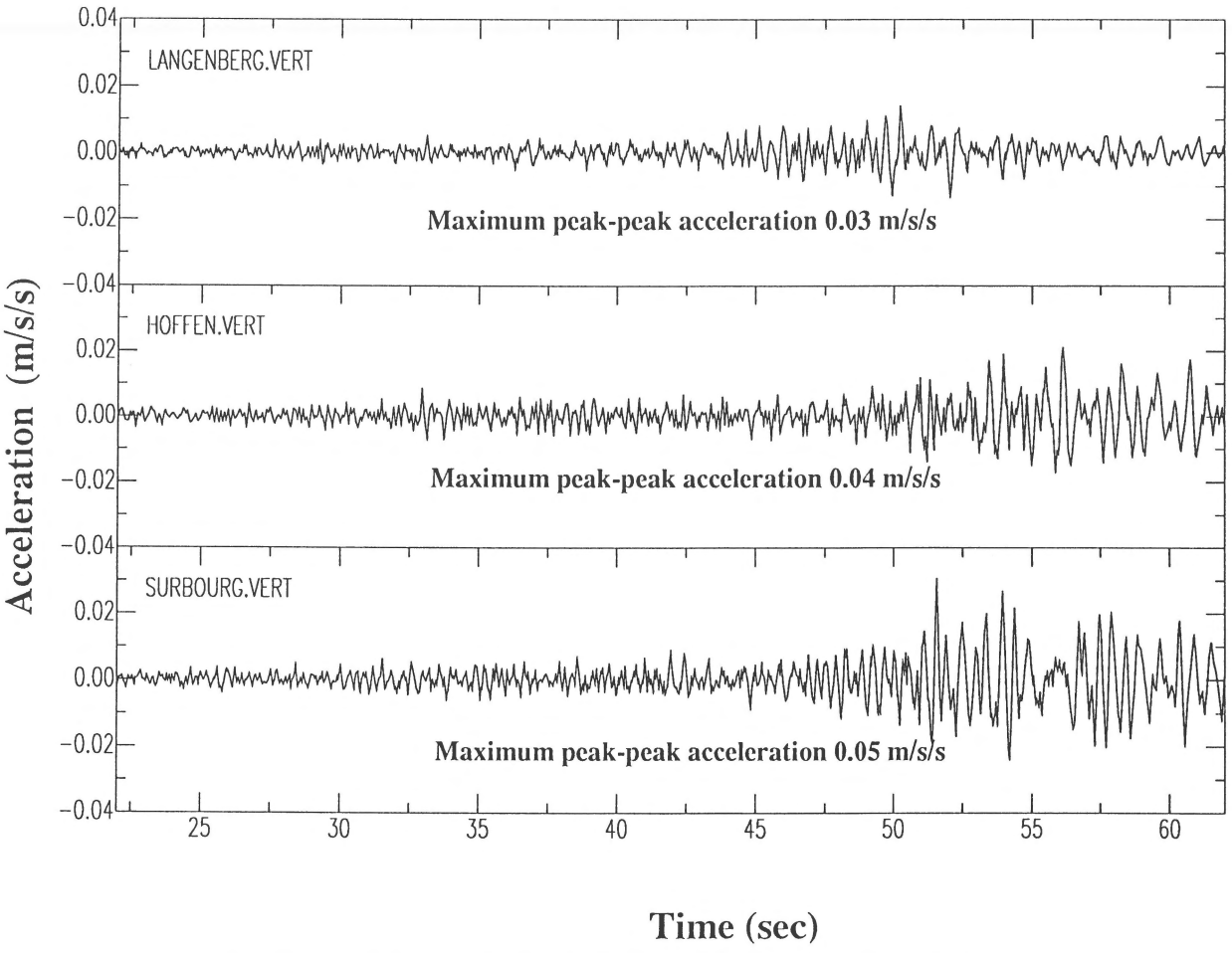

Fig. 3. Vertical component accelerometer recordings of the Roermond earthquake at Surbourg, Hoffen and Langenberg.

scaling laws have to be fulfilled. From the classical expressions for the seismic moment of the small reference event, m_o, and that of the large event, M_o, assuming the same stress drop for both events, we find the proportionality relation (Heaton & Hartzell 1989):

$$\frac{L}{l} = \frac{W}{w} = \frac{D}{d} = N \qquad (1)$$

In the above expression, capital letters refer to the large mainshock event, and lower case letters refer to the small event, L and l are fault lengths, W and w are fault widths, and D and d are final dislocations. Accordingly, the seismic moments m_o and M_o are scaled by the factor N^3:

$$M_o = N^3.m_o \qquad (2)$$

This means that we need a priori a summation of N^3 records to model the seismic motion associated with the large fault offset.

The simulated motion of the large event may be considered as a simple sum of time-lagged accelerograms with two main contributions: firstly, N source element time functions are added to build up the total dislocation D, and secondly, N^2 fault elements are necessary to cover the surface (Fig. 4). The simulated seismic motion may be written as:

$$S(t) = \sum_{n=1}^{N^2} \sum_{p=1}^{N} s(t - (p-1).t_d - \tau_n) \qquad (3)$$

where t_d is the small event rise time which describes the slip over the fault plane and τ_n is the time delay due to the rupture and the wave propagation.

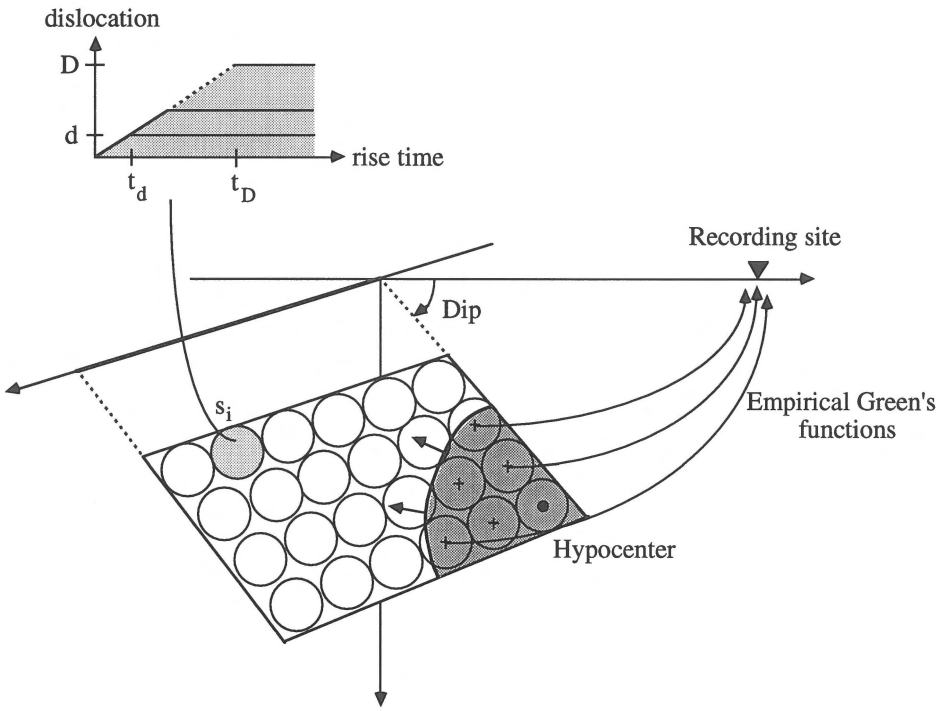

Fig. 4. 3-D source-receiver geometry. On each element (s_i) the slip function is modelled by a ramp dislocation d and rise time t_d. The rise time, the rupture propagation and the wave propagation are the different contributions to the time delays between the empirical Green's functions.

The method has been recently used by Bour & Cara (1995) for modelling the ground motion induced by medium sized events (M_L = 5.0 to 7.0) at several tens of kilometers from the epicenter.

Simulation of the main shock

Our data set provides a good opportunity to simulate the Roermond mainshock since a M_L = 3.6 aftershock was recorded on our network.

Using the record of the M_L = 3.6 aftershock as an empirical Green's function, we simulate the ground motion of the mainshock M_L = 5.8 at the station Surbourg. The two events are located 30 km from each other, at about 280 km and 250 km, respectively, from the station. The focal mechanism of the normal fault which ruptured during the mainshock has a strike of N127°E and a dip of 70° (Camelbeeck et al. 1994). The focal mechanism of the aftershock was also normal with strike N95°E and dip 80° (Pelzing 1994).

With an arbitrarily chosen rupture velocity c_r of 2800 m/s and a half-pulse duration of the small event $\tau_{1/2}$ of 0.2 sec, our estimate for the fault length, l, of the small event is 520 m. The seismic moment, M_o, of the mainshock is about 12.10^{16} N m, according to Camelbeeck et al. (1994). The seismic moment m_o for the small aftershock is taken to be 7.10^{13} N m. This value is derived from the empirical moment-magnitude law $\log_{10}(m_o) = 1.05\ M_L + 16.86$ given by Durst (1981) for magnitudes between 1 and 4.9 in the Swabian Jura region of southwest Germany. With a moment ratio of 1700, the fault surface is divided into 12 × 12 small faults in order to fulfill the scaling law (Eq. 2). Accordingly, the mainshock fault is modelled by a 6.2 km × 6.2 km square. With a stress drop of 1.2 MPa computed according to Kanamori & Anderson (1975) for a circular fault, we get a final dislocation D on the fault of 8.5 cm. We have fixed the slip velocity on the fault c_d to 100 cm/s, in agreement with the range of 10 to 100 cm/s mentioned by Aki & Richards (1980).

This yields a rise time t_D = 0.085 sec. Table 2 gives a summary of the source parameters used in our computation. These parameters are principally based on those given by several other investigations (Camelbeeck et al. 1994; Pelzing 1994). There are some uncertainties due to the fact that: i) the small source parameters are poorly determined, making it difficult to make an exact prediction of the source parameters of the large earth-

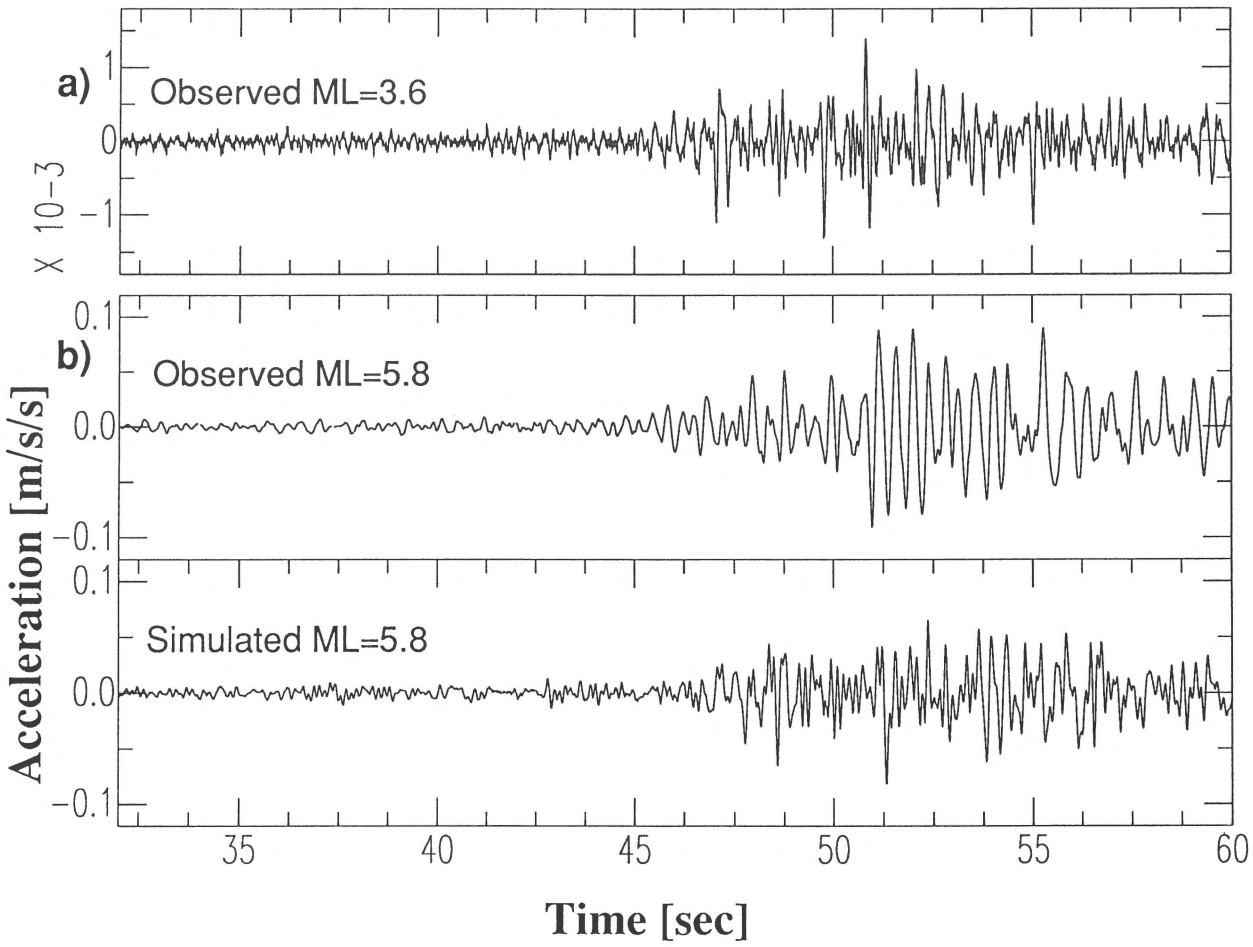

Fig. 5. a. Horizontal component accelerations observed at Surbourg for the M_L = 3.6 aftershock used as an empirical Green's function. b. Observed and simulated horizontal component accelerations for the M_L = 5.8 Roermond earthquake at Surbourg.

quake and ii) the aftershock was not at exactly the same location as the mainshock.

The simulated accelerogram presented in Fig. 5 corresponds to a rupture initiated near the lower northwestern corner of the fault plane furthest from the station, as suggested by Ahorner (1994). We assume a depth of about 16.7 km for this rupture initiation point. Figure 5 shows a reasonable agreement between the waveforms and good agreement of the amplitude of the observed acceleration and the simulated one. We obtain a maximum peak-to-peak acceleration of 0.17 m/s^2. The frequency content of the simulated and the observed accelerations are also in reasonable agreement. An example of this fit is shown on the 5% damping response spectra (Fig. 6). Thus the larger motion induced in a building (of natural frequency 2–3 Hz) located at 280 km from the Roermond epicenter would appear around a frequency of 2–3 Hz.

Conclusions

The data of the Roermond 1992 earthquake sequence recorded by our seismic network at Soultz-sous-Forêts are very interesting because they present a series of three-component accelerograms obtained at different sites, at moderate distances from the epicentral zone. These records also allow us to model the main event by the empirical Green's function approach.

The example was not ideal for the application of the method since the aftershock was located some 30 km away from the mainshock and on a fault with a dif-

Table 2. Source parameters used in the simulation of the $M_L = 5.8$ Roermond earthquake, with the small $M_L = 3.6$ aftershock as an empirical Green's function

Density	$\rho = 2600$ kg/m^3	
S-wave velocity	$\beta = 3750$ m/s	
Rupture velocity	$c_r = 2800$ m/s	
Slip velocity	$c_d = 1$ m/s	
	$M_L = 3.6$	$M_L = 5.8$
Seismic moment	$m_o = 7 \cdot 10^{13}$ Nm	$M_o = 1.2 \cdot 10^{17}$ Nm
Fault dimension	$1 = w = 520$ m	$L = W = 6.24$ km
Dislocation	$d = 7.1$ mm	$D = 8.5$ cm
Rise time	$t_d = 7 \cdot 10^{-3}$ sec	$t_D = 8.5 \cdot 10^{-2}$
Half pulse duration	$\tau_{1/2} = 0.2$ sec	
Fault plane (Φ-δ)	$127° \frac{1}{N} 70°$	
Hypocentral depth	$h_C = 16.7$ km	
Stress drop	$\Delta\sigma = 1.2$ MPa	

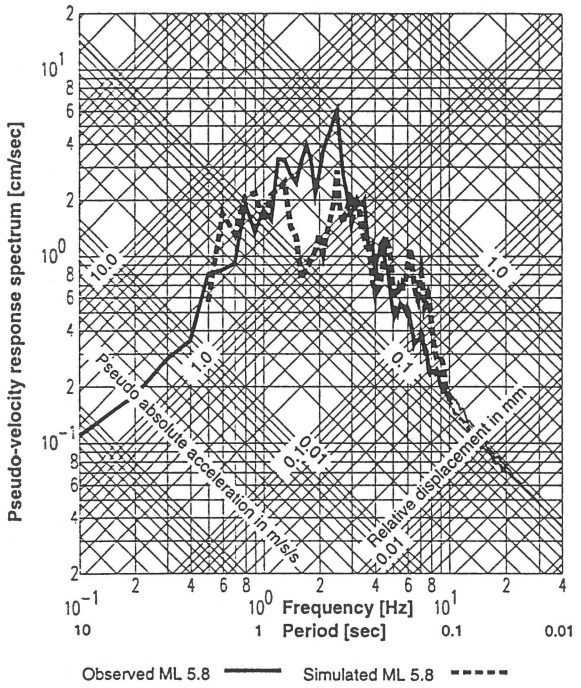

Fig. 6. Observed and simulated response spectra (5% damping) for the $M_L = 5.8$ Roermond earthquake. Due to the low-frequency electronic noise, the simulated signal was high-pass filtered at 0.5 Hz.

ferent orientation but the same mechanism. It is also important to stress that the uncertainties in the small event source parameters make it difficult to make any exact estimation of the large earthquake parameters. However, we have seen that in this situation the empirical Green's function method, using records of one of the smaller aftershocks, may be applied with some success to estimate the ground acceleration caused by the Roermond mainshock at a site in the Upper Rhine Graben.

Acknowledgements

We would like to thank Torild van Eck for details of the local velocity structure of the Lower Rhine Embayment, and Jean-Marie Holl, Jacky Sahr, Michel Frogneux and Hervé Blumentritt for technical assistance with the network.

References

Ahorner, L. 1994 Fault-plane solutions and source parameters of the 1992 Roermond earthquake, the Netherlands, and its stronger aftershocks from regional seismic data – Geol. Mijnbouw, this issue

Aki, K. & R.G. Richards 1980 Quantitative seismology: Theory and Methods. W.H. Freeman and Co., San Francisco, 812 pp

Bour, M. & M. Cara 1995 Test of the empirical Green's function method on moderate size earthquakes – Bull. Seismol. Soc. Am., in press

Camelbeeck, Th., T. van Eck, R. Pelzing, L. Ahorner, J. Loohuis, H.W. Haak, P. Hoang-Trong & D. Hollnack 1994 The 1992 Roermond earthquake, the Netherlands, and its aftershocks – Geol. Mijnbouw, this issue

Durst, H. 1981 Digitale Erfassung und Analyse der physikalischen Prozesse in den Erdbebenherden aus dem Bereich des Oberrheingrabens, Diplomarbeit, Karlsruhe University, 89 pp

Hartzell, S.H. 1978 Earthquake aftershocks as Green's function – Geophys. Res. Lett. 5: 1–4

Heaton, T.H. & S.H. Hartzell 1989 Estimation of strong ground motions from hypothetical earthquakes on the Cascadia subduction zone, Pacific Northwest PAGEOPH 129: 131–201

Kanamori, H. & D.L. Anderson 1975 Theoretical basis of some empirical relations in seismology – Bull. Seism. Soc. Am. 65: 1073–1095

Pelzing, R. 1993 Source parameters of the 1992 Roermond earthquake, the Netherlands, and some of its aftershocks recorded at the stations of the Geological Survey of Northrhine-Westphalia – Geol. Mijnbouw, this issue